Magnetic structures of $R_3Cu_4Sn_4$ (R = Pr and Nd)

2004 J. Phys.: Condens. Matter 16 45

(http://iopscience.iop.org/0953-8984/16/1/005)

INSTITUTE OF PHYSICS PUBLISHING JOURNAL OF PHYSICS: CONDENSED MATTER

J. Phys.: Condens. Matter **16** (2004) 45–52 PII: S0953-8984(04)69880-8

Magnetic structures of $R_3Cu_4Sn_4$ (R = Pr and Nd)

E Wawrzyńska[1], J Hernández-Velasco[2], B Penc[1] and A Szytuła[1]

[1] M Smoluchowski Institute of Physics, Jagiellonian University, Reymonta 4, 30-059 Kraków, Poland
[2] BENSC, Hahn-Meitner Institut, Glienicker Straße 100, D-14109 Berlin-Wannsee, Germany

E-mail: e.w@wp.pl

Received 2 October 2003, in final form 27 November 2003
Published 15 December 2003
Online at stacks.iop.org/JPhysCM/16/45 (DOI: 10.1088/0953-8984/16/1/005)

Abstract

Polycrystalline samples of $R_3Cu_4Sn_4$ (R = Pr and Nd) intermetallics were studied with neutron diffraction methods. Both of them crystallize in the orthorhombic structure of $Gd_3Cu_4Ge_4$-type. $Pr_3Cu_4Sn_4$ orders antiferromagnetically below the Néel temperature of about 11 K whereas $Nd_3Cu_4Sn_4$ does not order magnetically down to 1.5 K. In $Pr_3Cu_4Sn_4$ the magnetic moments are localized at the Pr atoms that occupy two non-equivalent 2d and 4e sublattices and order simultaneously at the Néel temperature forming a collinear magnetic order along the x-direction.

(Some figures in this article are in colour only in the electronic version)

1. Introduction

The rare earth intermetallic compounds are one of most attractive systems since they have very interesting magnetic and transport properties. Their magnetic properties are induced by a competition between two factors: exchange interactions of the RKKY type and the crystal electric field.

Recently the novel $R_3Cu_4X_4$ (R—rare earth elements, X = Si, Ge, Sn) compounds, which crystallize in the orthorhombic $Gd_3Cu_4Ge_4$-type crystal structure ($Immm$ space group, No. 71) [1], are the subject of intensive investigations. One of the reasons for this is the fact that in these structures rare earth atoms occupy two inequivalent sublattices. Results of magnetic and neutron diffraction measurements indicate differences of the magnetic properties of these compounds.

The $Ce_3Cu_4X_4$ (X = Ge, Sn) compounds are antiferromagnets, with the Néel temperature equal to 10.3 K for both. Below T_N three additional phase transitions are detectable in the specific heat measurements, while the neutron diffraction data give only two magnetic phases. The low-temperature phase in both compounds is collinear and antiferromagnetic, with the magnetic unit cell equal to the crystal one and with the Ce moments forming φ angles with the a-axis at 1.5 K and parallel to it at 3.8 K. Near the Néel temperature the Ce moments

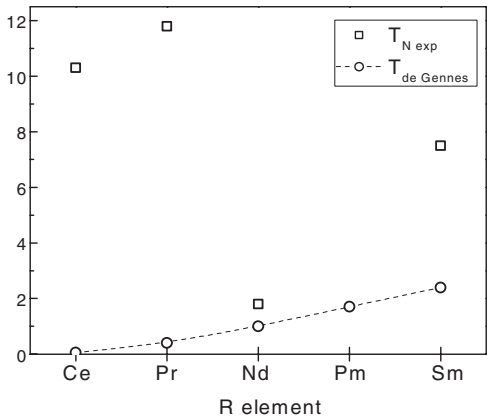

Figure 1. A comparison of the Néel temperatures observed in experiments and calculated from the de Gennes relation for the $R_3Cu_4Sn_4$ (R = Ce, Pr, Nd, Pm and Sm) compounds. The calculated values are normalized to the Néel temperature of $Gd_3Cu_4Sn_4$.

form modulated magnetic structures (the high-temperature phase). The values of the ordered Ce magnetic moments at different sites are different: close to the free Ce^{3+} ion value for the moments at the 2d sites (2.05(2) μ_B for X = Ge and 1.89(2) μ_B for X = Sn), and significantly reduced at the 4e sites (1.10(2) μ_B for X = Ge and 1.05(2) μ_B for X = Sn) [2]. The reduced value of the magnetic moment results from the superposition of two effects: the crystal electric field and the Kondo interactions. The magnetic and specific heat data for $Gd_3Cu_4Sn_4$ indicate three anomalies: a broad peak at 13 K, a second order phase transition at 8.2 K, and a first order transition at 6.5 K [3]. The neutron diffraction data for the $R_3Cu_4Sn_4$ (R = Tb–Er) compounds indicate the existence of complex magnetic structures at low temperatures [4]. The magnetic and specific heat data for the $R_3Cu_4Sn_4$ (R = Pr, Nd and Sm) compounds indicate that they are all antiferromagnets, with Néel temperatures equal to 11.8, 1.8 and 7.5 K, respectively. For $Sm_3Cu_4Sn_4$ an additional phase transition below the Néel temperature, at 5 K, is observed. For the Pr and Nd compounds, in contrast to the Ce, Sm and Gd compounds, no additional transitions below the Néel temperatures have been detected [5]. Large interatomic distances between the rare earth atoms indicate that the observed antiferromagnetic state is probably induced by the RKKY exchange interaction. In the RKKY model the critical temperature of the magnetic ordering is proportional to the de Gennes function [6]. The summarized data concerning this dependence (see figure 1) clearly indicate that this relation is not fulfilled for the Ce, Pr and Sm compounds.

A similar breakdown of the de Gennes scaling is also observed in the isostructural $R_3Cu_4Ge_4$ (R = Yb, Gd) compounds [7]. These observations indicate a strong exchange interaction between the Ce and Yb ions arising presumably from the 4f conduction band hybridization or crystal electric field effect.

In these compounds the rare earth ions occupy two different sublattices with two different local symmetries: the *mmm* symmetry for the 2d sites and the 2*mm* symmetry for the 4e sites; these experience a different crystal electric field. The ^{170}Yb Mössbauer effect for isostructural $Yb_3Cu_4Ge_4$ indicates that the quadrupolar interaction at the 4e sites has an axial character, while at the 2d sites it has a strong non-axial character [7]. Keeping in view the interesting magnetic behaviour observed for these compounds we have in this work investigated the crystal and magnetic structure of the $R_3Cu_4Sn_4$ (R = Pr and Nd) compounds, using neutron diffraction methods.

Table 1. The refined structural and magnetic parameters of the $R_3Cu_4Sn_4$ (R = Pr and Nd) compounds (space group *Immm* (No. 71)) obtained from the neutron diffraction data collected at 1.5 and 20 K for $Pr_3Cu_4Sn_4$ and at 1.5 and 7.5 K for $Nd_3Cu_4Sn_4$. Standard deviations are given in brackets.

Compound	$Pr_3Cu_4Sn_4$		$Nd_3Cu_4Sn_4$	
T (K)	1.5	20	1.5	7.5
a (Å)	14.983(4)	15.004(7)	14.975(5)	14.964(5)
b (Å)	6.980(2)	6.981(3)	6.976(2)	6.976(2)
c (Å)	4.561(1)	4.567(2)	4.546(2)	4.545(1)
V (Å^3)	477.0(2)	478.4(4)	474.8(3)	474.5(3)
x_R	0.119(1)	0.121(2)	0.127(1)	0.1322(9)
x_{Cu}	0.3330(5)	0.3323(7)	0.3344(6)	0.3347(5)
y_{Cu}	0.193(1)	0.196(2)	0.178(1)	0.186(1)
x_{Sn}	0.228(1)	0.223(2)	0.232(1)	0.222(1)
y_{Sn}	0.183(2)	0.174(3)	0.209(2)	0.185(2)
R_{Bragg} (%)	9.53	11.7	11.8	11.7
R_F (%)	6.44	9.33	8.21	8.40
μ_{2d} (μ_B)	2.9(2)	—	—	—
μ_{4e} (μ_B)	2.3(1)	—	—	—
R_{mag} (%)	17.2	—	—	—

2. Experimental procedure

Polycrystalline samples of the $R_3Cu_4Sn_4$ (R = Pr and Nd) compounds, each with total weight of about 5 g, were synthesized by arc melting of stoichiometric amounts of high purity elements (3N purity for R elements and 4N for Cu and Sn) in a Ti/Zr gettered argon atmosphere. The reaction products were annealed at 800 °C for a week.

Both samples were examined by x-ray powder diffraction (Cu Kα radiation) in order to check their purity. The peaks in the x-ray patterns were indexed in the orthorhombic $Gd_3Cu_4Ge_4$-type structure. In both samples the presence of the RCu_2Sn_2 (R = Pr and Nd for the $Pr_3Cu_4Sn_4$ and $Nd_3Cu_4Sn_4$ samples, respectively) phase in amounts of about 4(4)% was detected.

Neutron diffractograms were obtained on the E6 instrument at the BERII reactor, Hahn-Meitner Institut, Berlin. The incident neutron wavelengths were 2.4439(7) Å and the measurement temperatures ranged between 1.5 and 20 K. The neutron diffraction data were processed with a Rietveld-type programme, FULLPROF [8].

3. Results

3.1. Crystal structure

The neutron diffraction patterns recorded at 20 and 7.5 K for $Pr_3Cu_4Sn_4$ and $Nd_3Cu_4Sn_4$, respectively, as well as the x-ray patterns recorded at the room temperatures, confirmed that these compounds crystallize in the orthorhombic structure of $Gd_3Cu_4Ge_4$-type, described by the *Immm* space group (No. 71). In this structure the rare earth atoms occupy two sites: 2d $(1/2, 0, 1/2)$ and 4e $(x, 0, 0)$; the Cu atoms are situated at the 8n $(x, y, 0)$ positions and the Sn atoms are at the 4f $(x, 1/2, 0)$ and 4h $(0, y, 1/2)$ positions in the crystal unit cell. The determined values of the lattice parameters a, b and c as well as the positional parameters corresponding to the minimum of the reliability factor are listed in table 1.

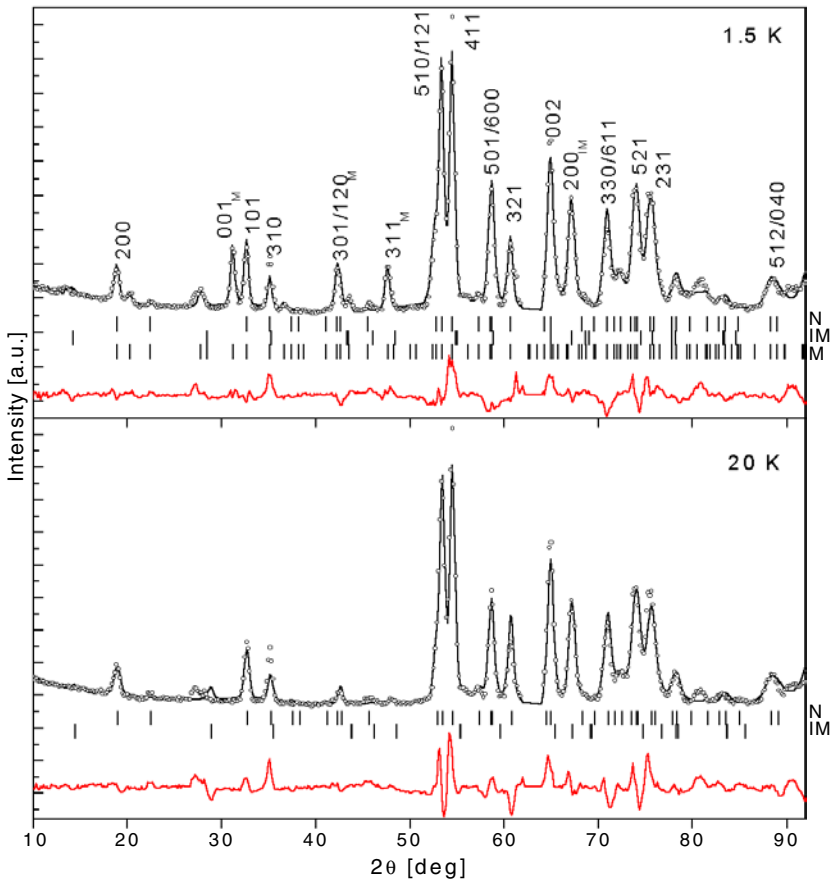

Figure 2. Neutron diffraction patterns of $Pr_3Cu_4Sn_4$ collected at 1.5 and 20 K. The circles represent the experimental points, the solid curves are calculated profiles for the model crystal and magnetic structures described in the text, and the differences between the observed and calculated intensities are at the bottom of each diagram. The vertical bars indicate the Bragg peaks of nuclear (N for $Pr_3Cu_4Sn_4$ and IM for the $PrCu_2Sn_2$ impurity phase) and magnetic (M) phase. The region around 63° was excluded due to the cryostat reflection.

3.2. Magnetic structure

3.2.1. $Pr_3Cu_4Sn_4$. The neutron diffraction patterns of $Pr_3Cu_4Sn_4$ recorded at low temperatures reveal the presence of additional peaks of magnetic origin. The pattern collected at 1.5 K is shown in figure 2. The analysis indicates that the Pr magnetic moments occupy two sites with the following positions in the crystal unit cell:

- the 4e sites: $\mathbf{M_1}$ $(x, 0, 0)$, $\mathbf{M_2}$ $(1 - x, 0, 0)$, $\mathbf{M_3}$ $((1/2) + x, 1/2, 1/2)$, $\mathbf{M_4}$ $((1/2) - x, 1/2, 1/2)$; and
- the 2d sites: $\mathbf{M_5}$ $(1/2, 0, 1/2)$, $\mathbf{M_6}$ $(0, 1/2, 0)$.

The analysis of the magnetic peak intensities leads to following conclusions.

- At 1.5 K the magnetic peaks can be indexed with the propagation vector $\mathbf{k} = (1, 1, 1)$ describing the ordering in both sublattices. The magnetic moments in both sublattices are aligned along the a-axis and their values are as follows: $\mu_{2d} = 2.9(2)\ \mu_B$ and

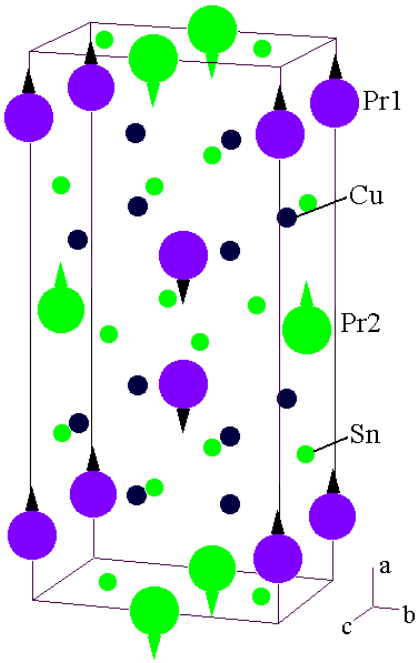

Figure 3. The magnetic structure of $Pr_3Cu_4Sn_4$ at 1.5 K.

Table 2. Basic vectors of the irreducible representations for **k** = (1, 1, 1) of the *Immm* space group in the 2d positions.

	(1/2, 0, 1/2)	(0, 1/2, 0)
τ_3	(1, 0, 0)	(−1, 0, 0)
τ_5	(0, 1, 0)	(0, −1, 0)
τ_7	(0, 0, 1)	(0, 0, −1)

Table 3. Basic vectors of the irreducible representations for **k** = (1, 1, 1) of the *Immm* space group in the 4e positions.

	$(x, 0, 0)$	$(1-x, 0, 0)$	$((1/2)+x, 1/2, 1/2)$	$((1/2)-x, 1/2, 1/2)$
τ_2	(1, 0, 0)	(−1, 0, 0)	(−1, 0, 0)	(1, 0, 0)
τ_3	(1, 0, 0)	(1, 0, 0)	(−1, 0, 0)	(−1, 0, 0)
τ_5	(0, 1, 0)	(0, 1, 0)	(0, −1, 0)	(0, −1, 0)
τ_6	(0, 0, 1)	(0, 0, −1)	(0, 0, −1)	(0, 0, 1)
τ_7	(0, 0, 1)	(0, 0, 1)	(0, 0, −1)	(0, 0, −1)
τ_8	(0, 1, 0)	(0, −1, 0)	(0, −1, 0)	(0, 1, 0)

$\mu_{4e} = 2.3(1)\ \mu_B$. The sequences of signs in the space of the crystal unit cell are antiferromagnetic in both of them: −+ for the 2d sublattice and ++−− for the 4e sublattice. The symmetry analysis supported by the MODY programme [9], carried out analogically as it was in our previous works [4, 10], allows three irreducible representations for the 2d sublattice and six irreducible representations for the 4e sublattice case, each of them appearing once (see tables 2 and 3). The fitted model is described by the τ_3 irreducible representation. $R_{mag} = 17.2\%$. The magnetic structure is shown in figure 3.

- At 20 K the Pr magnetic moments are not ordered.

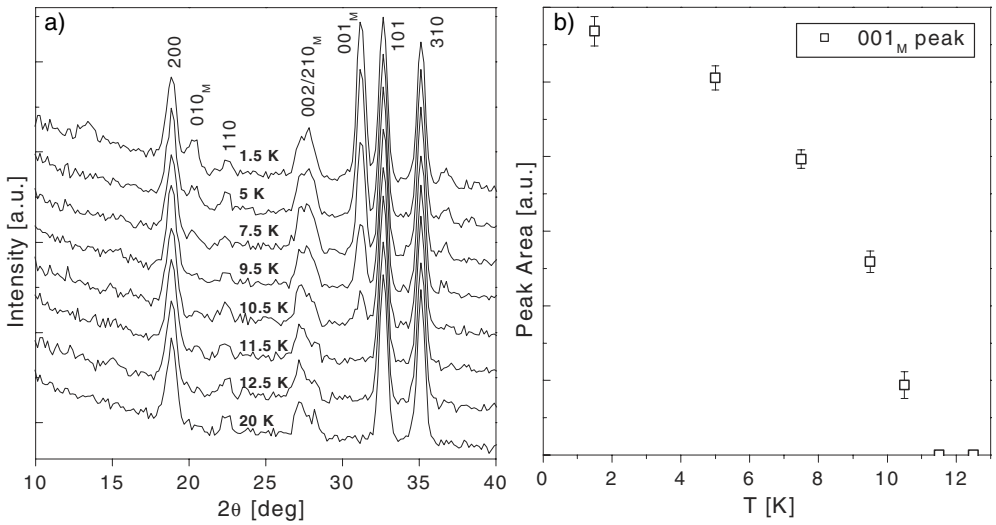

Figure 4. Part of the neutron diffraction patterns of $Pr_3Cu_4Sn_4$ measured at different temperatures (a) and the temperature dependence of the magnetic 001 peak intensity (b). The subscript M label the magnetic peaks.

Figure 4 shows the parts of the diffraction patterns of $Pr_3Cu_4Sn_4$ (angular range: 10°–40°) measured at different temperatures (part (a)) and the temperature dependence of the magnetic 001 peak intensity (part (b)). The Néel temperature may thus be estimated as equal to about 11 K.

3.2.2. $Nd_3Cu_4Sn_4$. The $Nd_3Cu_4Sn_4$ sample does not seem to order magnetically down to 1.5 K. The neutron diffraction pattern obtained at the temperature of 7.5 K as well as the 1.5–7.5 K difference pattern are shown in figure 5. The determined values of the lattice parameters a, b and c as well as the positional parameters corresponding to the minimum of the reliability factor are listed in table 1.

4. Discussion

Neutron diffraction data confirm that $Pr_3Cu_4Sn_4$ and $Nd_3Cu_4Sn_4$ crystallize in the orthorhombic $Gd_3Cu_4Ge_4$-type structure. $Pr_3Cu_4Sn_4$ reveals antiferromagnetic order at low temperatures and its Néel temperature can be estimated as equal to about 11 K. $Nd_3Cu_4Sn_4$ does not order magnetically down to 1.5 K. In $Pr_3Cu_4Sn_4$ the Pr magnetic moments in both non-equivalent 2d and 4e sublattices order simultaneously at the Néel temperature mentioned above and form a collinear antiferromagnetic order with the magnetic moments equal to 2.9(2) μ_B for the 2d sublattice and 2.3(1) μ_B for the 4e sublattice along the x-direction.

The determined magnetic structure of $Pr_3Cu_4Sn_4$ is similar to that observed in isostructural $Ce_3Cu_4Sn_4$ at low temperatures [2]. In $Pr_3Cu_4Sn_4$ the collinear magnetic order is stable while in $Ce_3Cu_4Sn_4$ the magnetic order changes to the modulated one near the Néel temperature.

The observed collinear magnetic ordering indicates a strong magnetocrystalline anisotropy connected with the crystal electric field. The differences of the values of the magnetic moments in different sublattices are connected with different crystal electric field effect, which influences the Pr^{3+} ions situated there. This is in a good agreement with specific heat and transport data [5].

The Pr magnetic moments values at the 2d and 4e sites are 91% and 72% of the free Pr^{3+} ion value (3.2 μ_B), respectively. This reduction may be connected with the strong influence

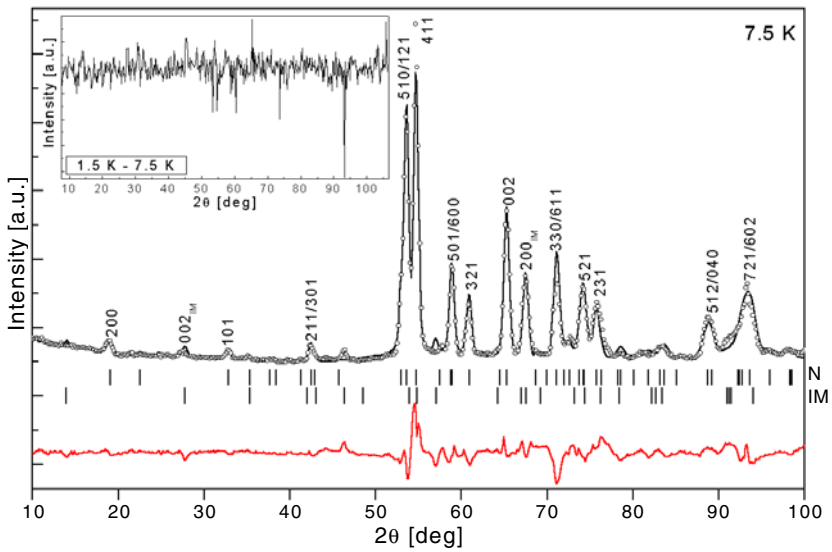

Figure 5. Neutron diffraction patterns of $Nd_3Cu_4Sn_4$ collected at 7.5 K. The circles represent the experimental points, the solid curves are calculated profiles for the model crystal and magnetic structures described in the text, and the differences between the observed and calculated intensities are at the bottom of the diagram. The vertical bars indicate the Bragg peaks of nuclear (N for $Nd_3Cu_4Sn_4$ and IM for the $NdCu_2Sn_2$ impurity phase). The inset shows the 1.5–7.5 K difference pattern.

of the crystal electric field and/or hybridization effect. The heat capacity data indicate that the crystal electric field splitting in $Pr_3Cu_4Sn_4$ is relatively low. The entropy at T_N is 6 J/Pr mol K and exceeds the theoretical value $R \ln 2$ (5.76 J/Pr mol K). The excess entropy arises from the thermal depopulation of the excited crystal field levels. A similar strong decrease of the magnetic moment values is observed in isostructural $Ce_3Cu_4Sn_4$ (1.89(2) μ_B for the 2d and 1.05(2) μ_B for the 4e sites). These values are 88.3% and 48% of the free Ce^{3+} ion value, respectively.

The absence of magnetic scattering in $Nd_3Cu_4Sn_4$ at 1.5 K resulted from the fact that the measurement temperature was near the Néel temperature (1.8 K).

5. Conclusions

The results presented in this work are a part of a broader research programme concerning investigations on the magnetic structures of the $R_3Cu_4X_4$ (R—rare earth element, X = Si, Ge, Sn) compounds. The determined magnetic structure of $Pr_3Cu_4Sn_4$ confirms the importance of the role of the crystal electric field for the stability of the magnetic ordering.

Acknowledgments

This work was supported by the European Commission under the IHP II Programme (project number: 466) and by the State Committee for Scientific Research in Poland within the confines of Grant 2P03B 113 23. EW and BP would like to express their gratitude to the management of the Berlin Neutron Scattering Centre for financial support and kind hospitality. Professor W Sikora from the University of Science and Technology in Cracow, Poland is kindly acknowledged for permitting the authors to use the MODY programme.

References

[1] Rieger W 1970 *Mon. Chem.* **101** 449
[2] Zaharko O, Keller L and Ritter C 2002 *J. Magn. Magn. Mater.* **253** 130
[3] Singh S, Dhar S K, Manfrinetti P and Palenzona A 2000 *J. Alloys Compounds* **298** 68
[4] Wawrzyńska E, Hernández-Velasco J, Penc B, Sikora W, Szytuła A and Zygmunt A 2003 *J. Phys.: Condens. Matter* **15** 5279
[5] Singh S, Dhar S K, Manfrinetti P and Palenzona A 2002 *J. Magn. Magn. Mater.* **250** 190
[6] de Gennes P G 1962 *J. Phys. Radium* **23** 510
de Gennes P G 1962 *J. Phys. Radium* **23** 630
[7] Dhar S K, Singh S, Bonville P, Mazumdar C, Manfrinetti P and Palenzona A 2002 *Physica* B **312/313** 846
[8] Rodriguez-Carvajal J 1993 *Physica* B **192** 55
[9] Sikora W 1994 *Proc. Symmetry and Structural Properties of Condensed Matter (Zajączkowo, Poland)* p 484
[10] Wawrzyńska E, Baran S, Leciejewicz J, Sikora W, Stüßer N and Szytuła A 2003 *J. Phys.: Condens. Matter* **15** 803